Available online at www.sciencedirect.com
SCIENCE DIRECT®
ELSEVIER
Materials Science in Semiconductor Processing 7 (2004) 1–6
MATERIALS SCIENCE IN SEMICONDUCTOR PROCESSING

Annealing effect for structural morphology of ZnO film on SiO_2 substrates

Hyoun Woo Kim*, Nam Ho Kim

School of Materials Science and Engineering, Inha University, 253 Yong-Hyun-Dong, Nam Ku, Incheon 402-751, Republic of Korea

Abstract

We have investigated the effect of annealing temperature on the structural morphology of ZnO thin films deposited on SiO_2 substrate by the RF magnetron sputtering method. We have used X-ray diffraction, scanning electron microscopy, and atomic force microscopy and have revealed that the grain size and surface roughness tends to increase and the *c*-axis orientation of ZnO thin film is enhanced by increasing the annealing temperature.

Keywords: Thin films; Sputtering; Structural properties

1. Introduction

Zinc oxide (ZnO) thin films have recently been extensively studied for surface acoustic wave (SAW) devices, optical wave-guides, and transparent conducting coatings [1]. Since the ZnO has a wide band gap of 3.37 eV, low-power threshold for optical pumping at room temperature, and UV emission resulted from a large exciton binding energy of 60 meV, they can be used as light emitting diodes (LED), photodetectors, electroluminescence devices and the next generation UV laser.

The ZnO films have been grown by various deposition methods, such as sputtering [2], sol–gel process [3], spray pyrolysis [4,5], pulsed laser deposition [6,7], ion beam deposition [8], plasma enhanced chemical vapor deposition (PECVD) [9], atomic layer deposition (ALD) [10], filtered cathodic vacuum arc technique [11], evaporation [12], metal-organic chemical vapor deposition (MOCVD) [13,14], and molecular beam epitaxy (MBE) [15].

Deposition of ZnO films on Si substrate pave the way for integration of devices with Si integrated circuits technology and amorphous substrates such as SiO_2 and glass substrate have obvious technological advantages and potential applications [16]. Also, the magnetron sputtering is a preferred technique due to its potential for low-temperature processing [17]. Although many researchers have grown ZnO films on sapphire substrates, there are not many reports on growing ZnO thin films on SiO_2 substrate by RF magnetron sputtering method. In this study, we deposit the ZnO thin film on SiO_2 substrates using the RF magnetron sputterer and investigated the effect of annealing temperature on the structural quality of ZnO thin films. Here, we reveal the effect of annealing temperature on three-dimensional ZnO film morphology using plan-view and cross-sectional scanning electron microscopy (SEM), X-ray diffraction analysis (XRD), and atomic force microscopy (AFM).

2. Experimental

Fig. 1 shows a schematic diagram of the RF sputtering system used in this study. The sputtering was carried out in an Ar (99.99% purity) gas atmosphere by supplying 300 W RF power at a frequency of 13.56 MHz. The flow rate of the Ar gas was set to

*Corresponding author. Tel.: +82-32-860-7544; fax: +81-32-862-5546.
E-mail address: hwkim@inha.ac.kr (H.W. Kim).

1369-8001/$ - see front matter
doi:10.1016/j.mssp.2003.12.001

30 sccm. The distance between target and substrate was about 80 mm.

The SiO_2 layer was thermally grown on the Si(1 0 0) substrate with a thickness of 60 nm. Before loading into the reactor, the substrate was cleaned in acetone for 10 min then rinsed by de-ionized water for 1 min. In this experiment, we have used a ZnO (99.99% purity) target with a diameter and a thickness of 75 and 6 mm, respectively.

The ZnO film was grown at a temperature of 25–200°C at a pressure of 5.0×10^{-2} Torr. The thickness of ZnO films ranged from 400 to 1300 nm. After RF magnetron sputtering, samples were annealed in a quartz tube furnace at the temperature of 600°C,

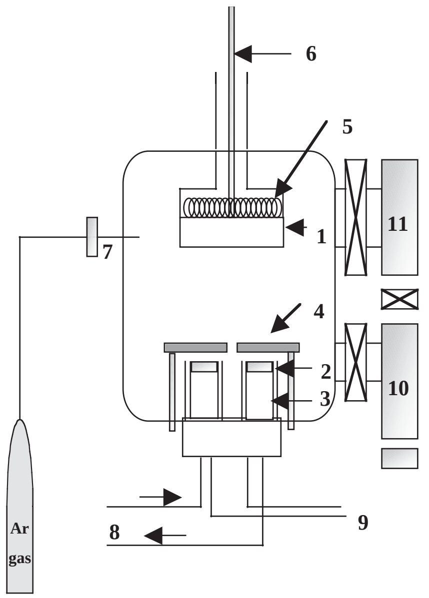

1. Substrate 2. Target 3. Magnetron 4. Shutter 5. Heater
6. Thermocouple 7. MFC 8. Cooling system 9. DC power supply
10. Rotary pump 11. Turbo pump

Fig. 1. Schematic diagram of RF magnetron sputtering system.

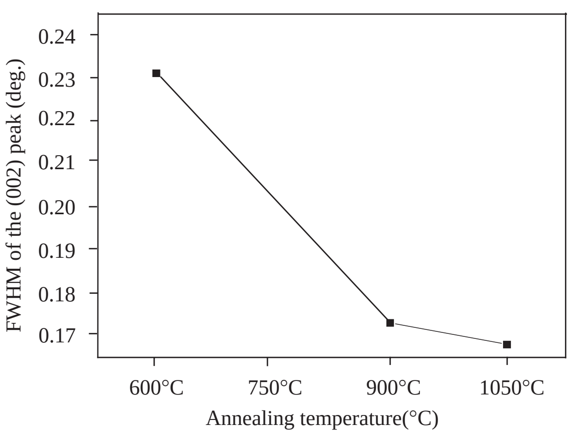

Fig. 2. Variation of the FWHM of the (0 0 2) diffraction peak by varying the annealing temperature in an ambient of oxygen.

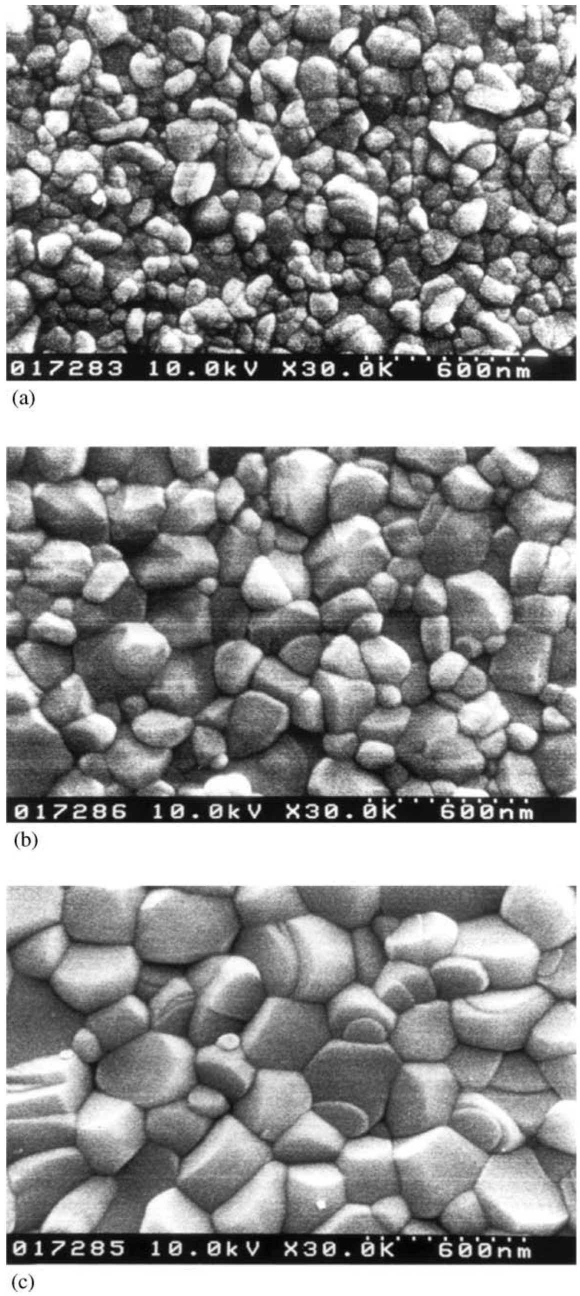

Fig. 3. Plain-view SEM images of ZnO film grown on SiO_2 substrate at the annealing temperature of (a) 600°C, (b) 900°C and (c) 1050°C.

900°C, and 1050°C in oxygen ambient for 1 h. Although no clear conclusion has been made on the effect of annealing ambient, several researchers maintained that the annealing in O_2 ambient is necessary for improving the structural properties of ZnO films [14,18]. In the oxygen ambient, the O_2 gas flow rate was set to 3 standard liter per min (slm). The structural characteristics of the films were analyzed by XRD using CuKa1 radiation ($\lambda = 0.154056$ nm) and SEM (Hitachi S-4200). The surface roughness was measured using a Digital Instruments Nanoscope III AFM.

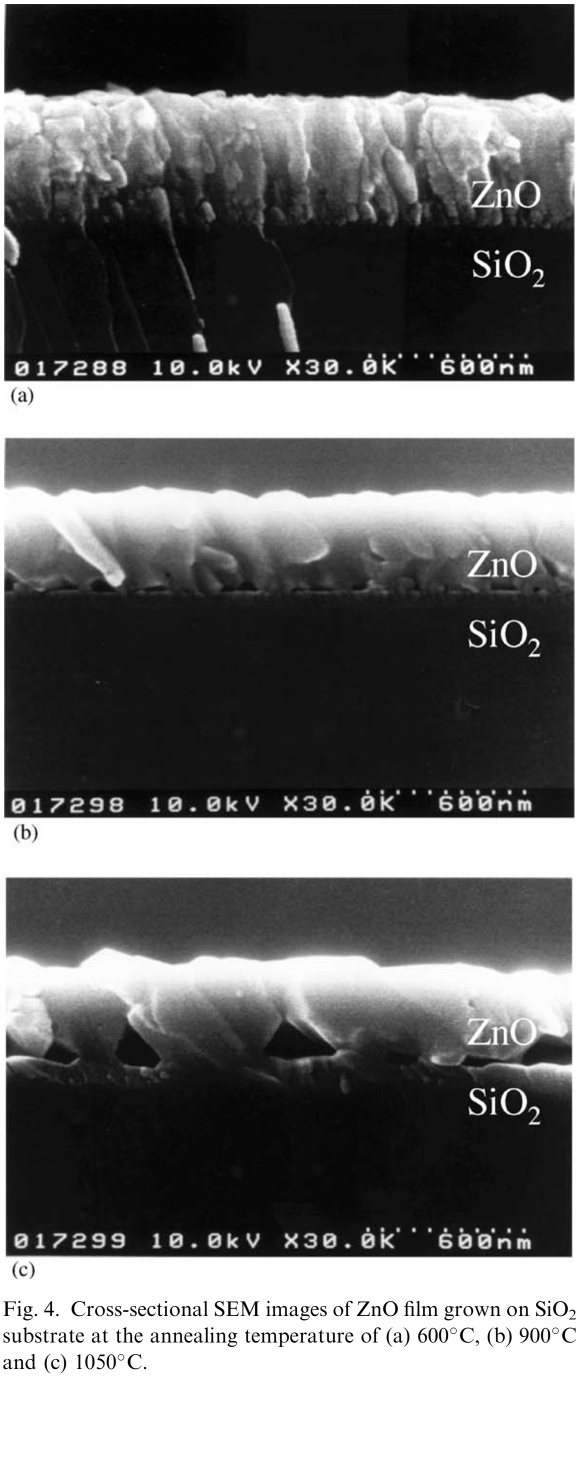

Fig. 4. Cross-sectional SEM images of ZnO film grown on SiO_2 substrate at the annealing temperature of (a) 600°C, (b) 900°C and (c) 1050°C.

3. Results and discussion

In order to investigate on the effect of thermal annealing on the crystallinity of ZnO thin film grown SiO_2 substrates, we have performed an XRD analysis. The ZnO film was grown at a temperature of 200°C and the thickness of ZnO films was set to be about 440–500 nm. In the θ–2θ XRD patterns of the ZnO thin film on SiO_2 substrate annealed in oxygen ambient for different annealing temperature ranging from 600°C to

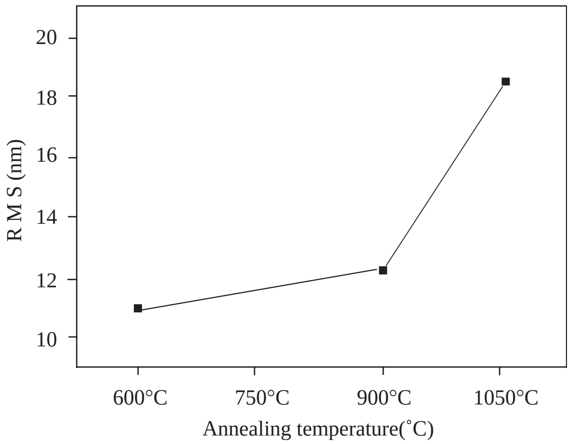

Fig. 5. Variation of RMS roughness measured by AFM, by varying the annealing temperature.

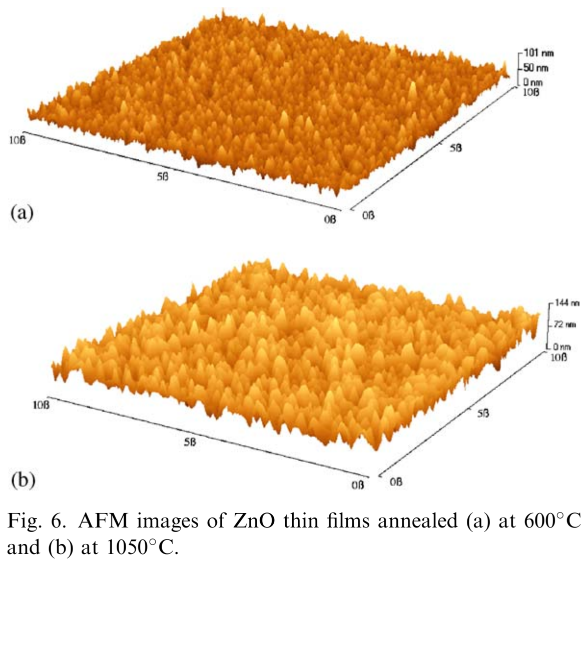

Fig. 6. AFM images of ZnO thin films annealed (a) at 600°C and (b) at 1050°C.

1050°C, the relative intensity of the ZnO (0 0 2) diffraction peak increases gradually by increasing annealing temperature (not shown here). We surmise that the c-axis orientation of ZnO films increases by increasing annealing temperature in the range of 600–1050°C.

Fig. 2 shows the full-width at half-maximum (FWHM) of the (0 0 2) diffraction peak according to the annealing temperature in oxygen ambient. The FWHM decreases by increasing the annealing temperature in the range 600–1050°C and becomes less than 0.2° by annealing at a temperature of 900–1050°C. The values of FWHM for the (0 0 2) diffraction peaks of ZnO films deposited on amorphous ZnO layer at 600°C, 900°C and 1050°C are 0.231°, 0.173° and 0.166°, respectively. For evaluating the mean grain size (D) of the films based on the XRD results, we applied the Scherrer formula [19]

$$D = 0.9\lambda/(B\cos\theta),$$

where λ, B, θ were X-ray wavelength (1.54056 Å), the FWHM of ZnO (0 0 2) diffraction peak, and the Bragg diffraction angle, respectively. By calculation, the mean grain sizes of the ZnO films are 37.6, 50.2 and 52.3 nm at 600°C, 900°C and 1050°C, respectively. Since the FWHM of the (0 0 2) diffraction peak is inversely proportional to the grain size of the film, the grain size of the ZnO thin film increases by increasing the annealing temperature.

Fig. 3 shows the plan-view SEM image of ZnO thin films annealed at 600°C, 900°C and 1050°C, revealing that the grain size becomes larger by increasing annealing temperature and this result agrees with the XRD analysis. Fig. 4 shows the cross-sectional view SEM images of ZnO thin films annealed at 600°C, 900°C and 1050°C, indicating that the magnitude of grain boundaries in ZnO thin film is reduced and thus we surmise that grains become larger by increasing the annealing temperature. Fig. 4c indicates that voids are generated in the bottom part of ZnO thin film at an annealing temperature of

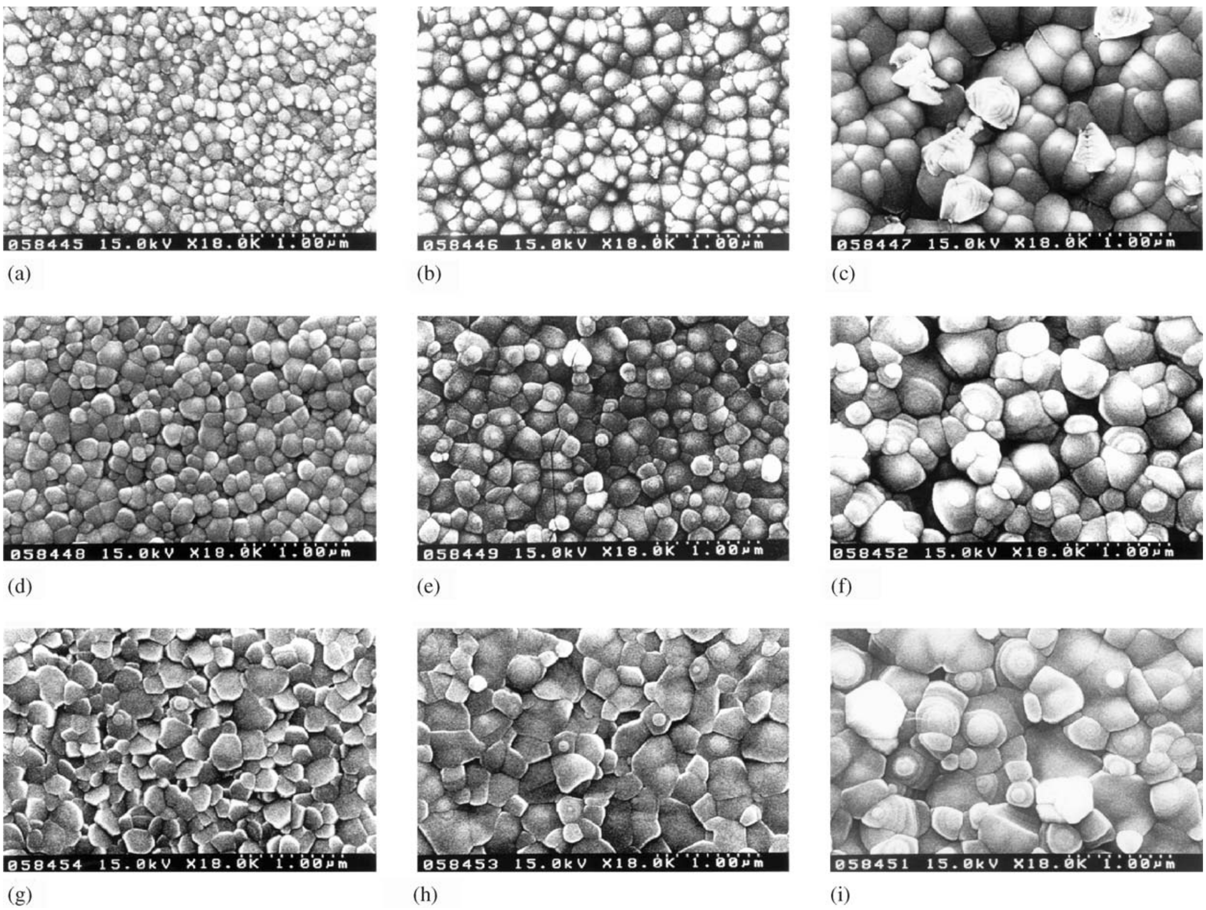

Fig. 7. Plain-view SEM images of ZnO film grown at room temperature with the annealing temperature of (a,b,c) 600°C, (d,e,f) 900°C and (g,h,i) 1050°C. The original thicknesses of ZnO films are (a,d,g) 400 nm, (b,c,h) 800 nm and (c,f,i) 1300 nm.

1050°C, possibly originating from the thermal stress at the interface. Furhther systematic study is needed to reveal the void generation mechanism.

Fig. 5 shows the variation of root mean square (RMS) roughness measured by AFM, by varying the annealing temperature. The AFM data indicate that the RMS roughness increases by increasing the annealing temperature, revealing that the ZnO surface roughness positively depends on the annealing temperature. Figs. 6a and b show the typical AFM images representing the surface morphology of ZnO thin film annealed at 600°C and at 1050°C, respectively. The AFM images indicate that the surface of ZnO thin film annealed at higher temperature (1050°C) is more rough than that annealed at lower temperature (600°C).

Gu et al. maintained that the atoms have enough diffusion activation energy to occupy the correct site in the crystal lattice and grains with the lower surface energy will become larger at high growth or annealing temperature [14]. Since the surface energy of the (0 0 0 2) orientation is lowest in the ZnO crystal [20], the growth orientation develops into one crystallographic direction of the low surface energy, leading to enlargement of grain size. We surmise that the surface becomes rougher with increasing the grain size due to the enlarged grain on top of the films, and thus the AFM images agree with the SEM images and the XRD data. Further study is necessary to reveal the detailed mechanism on the generation of large grain and rough interface at high-temperature annealing.

In order to investigate the effect of thickness on the structural characteristics with the changing annealing temperature, we have prepared ZnO films with various thicknesses by sputtering at room temperature and have annealed at 600°C, 900°C and 1050°C. Fig. 7 shows the plain-view SEM images of ZnO films, indicating that the grain size on top of the films increases with increasing the annealing temperature at a film thickness of 400–800 nm. However, when the original thickness of ZnO film is thick enough (1300 nm), the grain size does not increase with increasing the annealing temperature. The XRD analysis also indicates that the amount of positive dependence of grain size on annealing temperature decreases with increasing the film thickness (not shown here). Fig. 8 shows the cross-sectional SEM images of ZnO films annealed at 900°C with various film thicknesses. Since the ZnO grain size increases as the growth proceeds, the grain size on top of the film is bigger than that on the bottom of the film and thus the ZnO grain size on the top should increase with increasing the film thickness. Therefore, we surmise that the temperature effects is reduced for the thicker films not only due to the volume effect (i.e. the volume of ZnO films increases with increasing the film thickness and the thicker films is less affected by the same annealing treatment) but also due to the reduced grain growth velocity with enlarged grains [21].

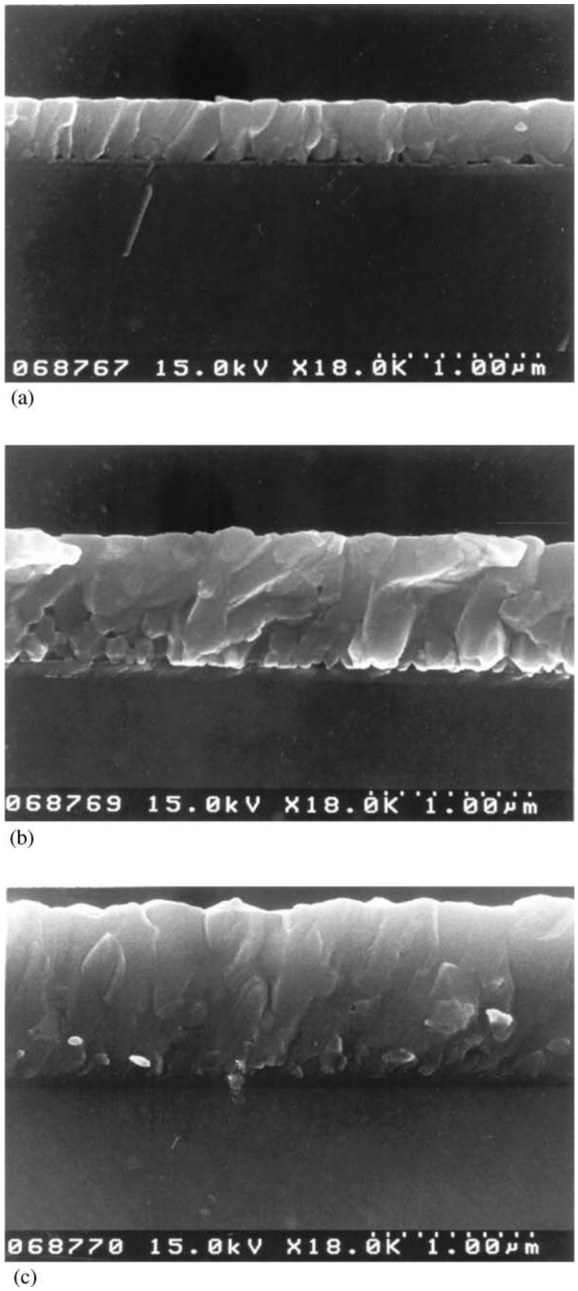

Fig. 8. Cross-sectional SEM images of ZnO film grown at room temperature with the annealing temperature of 900°C. The original thicknesses of ZnO films are (a) 400 nm, (b) 800 nm and (c) 1300 nm.

4. Conclusion

In summary, we have deposited the ZnO thin film on the SiO_2 substrate using the RF magnetron sputtering technique and have investigated annealing effects in oxygen ambient in the range of 600–1050°C. The SEM images and XRD data coincidently indicate that the grain size of ZnO film increases by increasing the annealing temperature for thin enough films. The XRD analysis indicates that the c-axis orientation of ZnO film is enhanced by increasing the annealing temperature. The AFM data indicate that the surface roughness increases by increasing the annealing temperature. However, the grain size does not significantly increase with increasing the annealing temperature for thicker films.

Acknowledgements

This work was supported by Grant No. R05-2001-000-00843-0 from the Basic Research Program of the Korea Science and Engineering Foundation.

References

[1] Yamamoto T, Shiosaki T, Kawabata A. J Appl Phys 1980;51:3113.
[2] Ondo-Ndong R, Pascal-Delannoy F, Boyer A, Giani A, Foucaran A. Mater Sci Eng 2003;B97:68.
[3] Lee J-H, Ko K-H, Park B-O. J Cryst Growth 2003;247:119.
[4] Ayouchi R, Martin F, Leinen D, Ramos-Barrado JR. J Cryst Growth 2003;247:497.
[5] Lokhande BJ, Patil PS, Uplane MD. Mater Lett 2002;57:573.
[6] Zeng JN, Low JK, Ren ZM, Liew T, Lu YF. Appl Surf Sci 2002;197:362.
[7] Kim H, Horwitz JS, Qadri SB, Chrisey DB. Thin Solid Film 2002;420:107.
[8] Whangbo SW, Jang HK, Kim SG, Cho MH, Jeong KH, Whang CN. J Korean Phys Soc 2000;37:456.
[9] Li BS, Liu YC, Shen DZ, Zhang JY, Lu YM, Fan XQ. J Cryst Growth 2003;249:179.
[10] Yamada A, Sang B, Konagai M. Appl Surf Sci 1997;112:216.
[11] Xu XL, Lau SP, Chen JS, Sun Z, Tay BK, Chai JW. Mater Sci Semicond Proc 2001;4:617.
[12] Gordillo G, Calderon C. Sol Energy Mater Sol Cells 2001;69:251.
[13] Du G, Wang J, Wang X, Jiang X, Yang S, Ma Y, Yan W, Gao D, Liu X, Cao H, Xu J, Chang RPH. J Cryst Growth 2003;243:439.
[14] Ye J, Gu S, Zhu S, Chen T, Hu L, Qin F, Zhang R, Shi Y, Zheng Y. J Cryst Growth 2002;243:151.
[15] Iwata K, Fons P, Niki S, Yamada A, Matsubara K, Nakahara K, Tanabe T, Takasu H. J Cryst Growth 2000;214/215:50.
[16] Guha S, Bojarczuk NA. Appl Phys Lett 1998;73:1487.
[17] Lu YM, Hwang WS, Liu WY, Yang JS. Mater Chem Phys 2001;72:269.
[18] Ogata K, Sakurai K, Fujita Sz, Fujita Sg, Matsushige K. J Cryst Growth 2000;214/215:312.
[19] Cullity BD. Elements of X-ray diffraction, 2nd ed. Reading, MA: Addison-Wesley; 1978.
[20] Fujimura N, Nishihara T, Goto S, Xu J, Ito T. J Cryst Growth 1993;130:269.
[21] Porter DA, Easterling KE. Phase transformations in metals and alloys. New York: Van Nostrand Reinhold; 1981.